



# Ruthenium red as an effective blocker of calcium and sodium currents in guinea-pig isolated ventricular heart cells

<sup>1</sup>Claire O. Malécot, Virginie Bito & Jorge A. Argibay

Physiologie des Cellules Cardiaques et Vasculaires, CNRS UMR 6542, Faculté des Sciences, Parc de Grandmont, 37200 Tours, France

- 1 The effect of ruthenium red on calcium and sodium currents was studied in guinea-pig isolated ventricular heart cells with the whole cell patch-clamp technique.
- 2 Ruthenium red very efficiently blocked the L-type calcium current in a dose-dependent manner. A significant block was observed for concentrations as low as 0.3  $\mu\text{M}$ . Analysis of the dose-response curve with the logistic equation indicated an  $\text{EC}_{50}$  of 0.8  $\mu\text{M}$ , a maximum inhibition of 85% reached at 5  $\mu\text{M}$ , and a coefficient of 2.37.
- 3 There was no shift in the voltage-dependence of the Ca current activation, nor in that of its steady-state inactivation determined with a 1 s prepulse. However, removal of Ca current inactivation at positive voltage was considerably reduced in the presence of concentrations of ruthenium red above 1  $\mu\text{M}$ . A slowing of the time-course of inactivation of the Ca current was also observed.
- 4 At 10  $\mu\text{M}$ , a concentration generally used to block the sarcoplasmic Ca release channels or the mitochondrial Ca uptake, ruthenium red blocked  $26.7 \pm 4.3\%$  ( $n=8$ ) of the sodium current, and slowed its inactivation time-course. No effect was observed on the voltage-dependence of the current activation or inactivation. The peak sodium current was also decreased at a 10 times lower concentration by  $7.6 \pm 2.7\%$  ( $n=3$ ).
- 5 Thus, at concentrations used to assess intracellular Ca movements, ruthenium red induced in heart cells a significant block of both Ca and Na channels.

**Keywords:** Ruthenium red; isolated heart cells; Ca current; Na current; whole-cell patch-clamp; ion channel block

## Introduction

Ruthenium red (structural formula  $(\text{NH}_3)_3\text{Ru}-\text{O}-\text{Ru}(\text{NH}_3)_4-\text{O}-\text{Ru}(\text{NH}_3)_3\text{Cl}_6$ ) is a synthetic crystalline inorganic polycationic dye which has been found to be useful for electron microscopy of cells and tissues as it strongly reacts with phospholipids and fatty acids and binds to acidic mucopolysaccharides (Luft, 1971). Ruthenium red staining of intracellular organelles and structures seemed to depend on the time of exposure to this agent, as well on the concentration used (Luft, 1971; Gupta *et al.*, 1988; Leperre *et al.*, 1995). Diffusion of ruthenium red into skeletal muscle fibre segments was found to be extremely slow (Feldmeyer *et al.*, 1993). However, it has been suggested that the entry of ruthenium red into a muscle cell might be coupled to that of calcium. Luft (1971) has shown that the peculiar distribution of ruthenium red in the tubules and in the adjacent sarcoplasmic sacs of the triads might be the consequence of a reversible change in plasma membrane permeability, and that ruthenium red appears to move selectively along a pathway postulated for calcium. More recently, Viele and Betz (1995) showed that the uptake of ruthenium red by endothelial cells during stimulation was blocked in the presence of the calcium channel blocker flunarizine, suggesting that functional calcium channels might be a route for ruthenium red to enter the cell. One interesting property of ruthenium red is its reported protective effect in ischaemia. In fact, in a cardiac model of ischaemia-reperfusion, ruthenium red was found to prevent cell damage and improve the contractility recovery, probably by preventing mitochondrial calcium overload and free radicals production (Grover *et al.*, 1990; Figueredo *et al.*, 1991; Benzi & Lerch, 1992; Tan, 1993; Leperre *et al.*, 1995;

Miyamae *et al.*, 1996). A direct effect of ruthenium red on the heart contractile apparatus might also partly explain this improved contractility recovery. Indeed, the calcium sensitivity of the myofilaments in the presence of ruthenium red has been shown to be either increased (chemically skinned rat papillary muscle treated with 2 or 10  $\mu\text{M}$  ruthenium red; Zhu & Nosek, 1992) or decreased (skinned ferret papillary muscle exposed to 50  $\mu\text{M}$  ruthenium red; Tanaka *et al.*, 1997). Besides these effects, ruthenium red has been shown to block the Ca release channels of the sarcoplasmic reticulum (Chamberlain *et al.*, 1984; Nagasaki & Fleischer, 1989; Mack *et al.*, 1992; Ma, 1993; Vites & Pappano, 1994; Ding & Kasai, 1996) and the mitochondrial Ca uptake (Moore, 1971; Vasington *et al.*, 1972; Sordahl, 1975; Rizzuto *et al.*, 1987).

Very little is known on the possible effects of ruthenium red on sarcolemmal ion channels, especially in the heart (for which no voltage-clamp data are available in the literature, to our knowledge). A few studies have nevertheless shown that ruthenium red blocks Ca channels in chromaffin cells (all types of Ca channels; Gomis *et al.*, 1994), snail neurones (Stimers & Byerly, 1982), and the N- and P-type (but not the L-type) Ca channels in chicken brain and rat synaptosomes (Hamilton & Lundy, 1995). In smooth muscle cells of the guinea-pig ileum, the calcium current is either decreased (Zholos *et al.*, 1991) or not affected (Gagov *et al.*, 1994). A slowing of Na current inactivation in the presence of ruthenium red has also been observed without or with a partial inhibitory effect in snail neurones (Stimers & Byerly, 1982), rat and frog myelinated nerve (Neumcke *et al.*, 1987) and neuroblastoma cells (Nosyreva *et al.*, 1988). However, chromaffin cells Na channels are not affected (Gomis *et al.*, 1994). Recently, in a short study, Griffiths (1997) showed that,

<sup>1</sup> Author for correspondence.

in single rat heart cells, the decrease in mitochondrial calcium in the presence of ruthenium red was accompanied by a decrease in systolic calcium and cell shortening. This result might be taken as an indication that ruthenium red may affect calcium entry also in heart cells. This hypothetical decreased calcium influx might also contribute to the protective effect of ruthenium red in ischaemia-reperfusion (see above). Therefore, we have investigated its effects on the L-type Ca current and on the Na current in freshly isolated ventricular heart cells of the guinea-pig, by use of the whole-cell patch-clamp technique. We showed here that ruthenium red, at concentrations generally used to assess intracellular Ca movements, is a very efficient blocker of heart sarcolemmal Ca channels and that it also affects Na channels.

## Methods

### Cell isolation

Guinea-pig heart cells were enzymatically isolated from the left ventricle as described elsewhere (Le Guennec *et al.*, 1993). The experimental procedure was performed in accordance with the French ethical guidelines. Dissociated cells were placed in a small chamber, on the stage of an inverted microscope (Olympus IX70, Tokyo, Japan), continuously superfused by gravity with normal Tyrode solution containing (in mM): NaCl 140, KCl 5.4, MgCl<sub>2</sub> 1, CaCl<sub>2</sub> 1.8, NaH<sub>2</sub>PO<sub>4</sub> 0.33, HEPES buffer 10 and glucose 11; pH adjusted to 7.3 with NaOH.

### Electrophysiological recordings and analysis

The whole-cell patch-clamp technique was used to study the L-type calcium and the sodium currents at room temperature (22–25°C). To record the ionic currents, the cells were locally superfused by gravity (small capillaries positioned within 50 µm of the cell and allowing fast solution changes) with a solution blocking all ionic currents except that under study. For the calcium current experiments, the solution contained (in mM): TEACl 140, CaCl<sub>2</sub> 1.8, MgCl<sub>2</sub> 1, HEPES buffer 10 and glucose 11 (pH 7.3 with TEAOH). For the sodium current recordings, the solution contained (in mM): NaCl 30, TEACl 110, CaCl<sub>2</sub> 1, MgCl<sub>2</sub> 1, CoCl<sub>2</sub> 2, GdCl<sub>3</sub> 0.1, HEPES buffer 10 and glucose 11 (pH 7.3 with TEAOH). The intracellular pipette solution contained (in mM): CsCl 110, TEACl 30, MgCl<sub>2</sub> 1, MgATP 5, EGTA 10 and HEPES buffer 10 (pH 7.3 with TEAOH).

Patch pipettes ( $2.8 \pm 0.08$  MΩ, mean  $\pm$  s.e.,  $n = 57$ ; range 1.0–3.7 MΩ) were pulled from thick wall borosilicate glass capillaries (Clark Electromedical Instruments, Reading, U.K.) with a Narishige PB7 puller (Narishige, Tokyo, Japan) and were coated with dental wax to decrease their capacitances. An Axopatch 200A amplifier (Axon Instruments Inc., Foster City, CA, USA), connected to a Pentium 75 computer equipped with pClamp 6.0.3 software (Axon Instruments), through a Digidata 1200A interface (Axon Instruments), was used to control voltage and record currents from a holding potential (HP) of  $-110$  mV (Na current) or  $-80$  mV (Ca current). Data were analysed with Clampfit. The pipette and cell capacitances were compensated. In order to have an adequate control of the membrane voltage and to improve the clamp speed, care was taken to select relatively small cells (membrane capacitance  $C_m = 84.2 \pm 3.7$  pF,  $n = 57$ ; range 31–136 pF) to carry out the experiments, especially for those dealing with the sodium current ( $C_m = 70.3 \pm 6.3$  pF,  $n = 13$ ). Cells for which the membrane capacitance varied by more than 2% during the

time course of the experiments were discarded and not included in the analysis. The series resistance was also compensated by 80%; this value was chosen to avoid saturation of the electrical circuit of the Axopatch 200A with the large voltage commands used. The mean time constant of the clamp speed, determined from the residual series resistance after compensation ( $1.44 \pm 0.07$  MΩ,  $n = 57$ ) and the mean cell capacitance, was  $123.9 \pm 9.0$  µs ( $n = 57$ ). Thus, in most of the cells, more than 98% of the command voltage was seen by the membrane in less than 500 µs. The data were acquired at 6.7 kHz (Ca current experiments) or 25 kHz (Na current experiments) and filtered with an 8-pole lowpass Bessel filter at 5 kHz. A P/5 subtraction protocol (Bezanilla & Armstrong, 1977), used to remove linear capacitive currents during the Na current experiments, was applied either before or after the test pulse or before the conditioning pulse (no difference found) from a subholding potential of  $-120$  mV. This was made possible because of the linearity of the residual leak current between  $-140$  mV and  $+20$  mV in the presence of the blockers of ionic currents used in our recording conditions. For the calcium current experiments, the P/5 subtraction protocol was not used. Calcium and sodium currents were measured as the maximum peak inward current. When quantified, their amplitudes are normalized to the cell capacitance and are expressed in pA/pF. Other data are expressed as mean values  $\pm$  s.e. of the mean observed in  $n$  different cells.

### Drugs

As stated by Luft (1971), ruthenium red obtained from commercial sources contains impurities, mostly ruthenium brown (an oxidation product of ruthenium red) and ruthenium violet. Although this author described a method to purify ruthenium red, no attempt was made to do so in our study. Ruthenium red (Sigma Chemicals, St Quentin Fallavier, France) was prepared as a 10 mM stock solution (with a molecular weight of 786.35) in distilled water and directly added to the superfusing saline at the final desired concentration. Because the batch of ruthenium red we used was  $\approx 50\%$  pure, the actual concentration of ruthenium red in solution was probably  $\approx 50\%$  of that indicated in this paper.

## Results

### Effect of ruthenium red on the L-type calcium current

The effects of ruthenium red were first tested on the L-type calcium current ( $I_{Ca}$ ) at a concentration blocking the sarcoplasmic reticulum Ca channels ( $10$  µM) and at a much lower concentration ( $0.5$  µM), supposedly not affecting these channels. Figure 1A shows the time course of the effect of two successive short applications of  $0.5$  µM ruthenium red on the amplitude of the peak  $I_{Ca}$  elicited by applying 150 ms depolarizing pulses from  $-80$  to  $0$  mV at  $0.1$  Hz. The ruthenium red effect appeared to be multi-phasic: an initial short period of fast block was followed by a transient re-increase in  $I_{Ca}$  amplitude and then by a second period of slower decrease of  $I_{Ca}$ . These effects were fully reversible upon washout of the drug, and a second application of ruthenium red had basically the same effects, except that the transient increase in  $I_{Ca}$  was much less marked, being almost absent. The transient increase of  $I_{Ca}$ , when it occurred, was always concomitant with a transient apparent slowing of the kinetics of inactivation of the current (not shown). This last effect

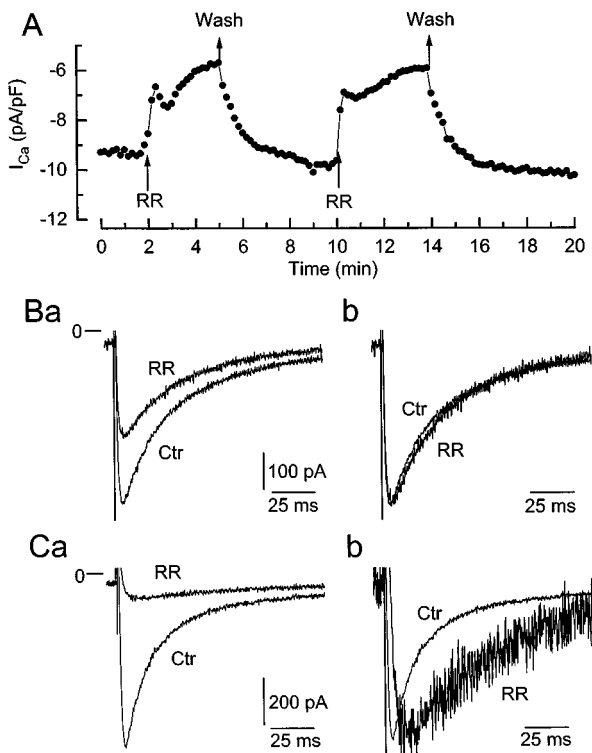


**Figure 1** Time-course of the effects of two successive short applications of 0.5  $\mu$ M ruthenium red (RR) on the amplitude of the peak inward calcium current elicited with 150 ms depolarizing pulses applied from  $-80$  to  $0$  mV (cell B7N06,  $C_m = 136$  pF). (B,C) Typical current recordings showing the inhibitory effect of 0.5  $\mu$ M (B) and of 10  $\mu$ M (C) ruthenium red on the calcium current elicited by applying a 150 ms depolarizing pulse from  $-80$  to  $0$  mV in two different cells (F7N06,  $C_m = 83.8$  pF, and B7O20,  $C_m = 106$  pF, respectively). In (Ba) and (Ca) are shown the actual current traces and in (Bb) and (Cb) current traces normalized to their maximum, so that the slowing of the kinetics of the Ca current in the presence of ruthenium red could be seen better.

might be sufficient in itself to explain the increase in the peak  $I_{Ca}$ .

Figure 1B and C show typical recordings of the steady-state effects of a low (0.5  $\mu$ M) and of a high (10  $\mu$ M) concentration of ruthenium red on the calcium current ( $I_{Ca}$ ) elicited under the same conditions as in Figure 1A. At a low concentration, ruthenium red significantly decreased the amplitude of  $I_{Ca}$  (Figure 1Ba) without much affecting its time course, as illustrated in Figure 1Bb where current traces have been normalized to their maximum. However, at a high concentration, not only  $I_{Ca}$  was markedly decreased (Figure 1Ca), but both the activation and inactivation kinetics were slowed, as seen in Figure 1Cb in which the normalized current traces are presented. Thus, ruthenium red appears to be an effective blocker of  $I_{Ca}$ .

The blocking effects of ruthenium red were also studied in the whole potential range corresponding to the activation of the calcium current. Figure 2Aa and Figure 2Ba show typical examples of the current-voltage relationships of  $I_{Ca}$  in control conditions and in the presence of 0.5  $\mu$ M and 1.5  $\mu$ M ruthenium red, respectively. In control conditions,  $I_{Ca}$  activated at around  $-40$  mV, reached its maximum at  $0$  mV and gradually decreased toward almost zero at around  $+70$  mV. In the presence of ruthenium red, the decrease of  $I_{Ca}$  was observed throughout the explored potential range, without any changes in the threshold potential, voltage at

which  $I_{Ca}$  reached its maximum amplitude, or apparent reversal potential, suggesting a lack of voltage-dependence in the inhibition by ruthenium red. On average,  $I_{Ca}$  was decreased at  $0$  mV by  $23.8 \pm 0.9\%$  ( $n = 5$ ) and by  $66.3 \pm 2.1\%$  ( $n = 4$ ) in the presence of 0.5  $\mu$ M and of 1.5  $\mu$ M ruthenium red, respectively.

The voltage-dependence of the steady-state inactivation of  $I_{Ca}$  was determined with a classical double pulse protocol consisting of a series of one second inactivating prepulses applied from  $-100$  mV to various potentials, and of a 400 ms test pulse from  $-100$  mV to  $0$  mV applied 8 ms after the termination of the inactivating prepulse, as indicated in the legend of Figure 2. Examples of the normalized data obtained during the test pulse are given for two ruthenium red concentrations in Figure 2Ab and Bb, for the same cells as those in Aa and Ba of Figure 2. In control conditions, inactivation of  $I_{Ca}$  with voltage started for potentials more positive than  $-50$  mV, was maximal in the range  $-10$  to  $+20$  mV, and then declined for potentials positive to  $+20$  mV. In the presence of ruthenium red,  $I_{Ca}$  inactivation with voltage was already significant for potentials negative to  $-40$  mV and almost unchanged between  $-40$  to  $+20$  mV. For potentials positive to  $+20$  mV, no effect occurred at the lower concentration (0.5  $\mu$ M, Figure 2Ab), whereas the decline in inactivation was markedly reduced at the higher concentration (1.5  $\mu$ M, Figure 2Bb). At this last concentration, total inactivation was less complete, as the non-inactivating component was increased from about 11.5% to about 16.5%. These effects of ruthenium red on the voltage-dependence of the steady-state inactivation of  $I_{Ca}$  were consistently observed in each cell.

To quantify more precisely the concentration-dependent inhibition of  $I_{Ca}$  by ruthenium red, a dose-response curve was determined and this is shown in Figure 3. Each data point corresponds to the mean inhibition of  $I_{Ca}$  observed on  $n$  cells, following a single application of ruthenium red at the indicated concentration. Fit of the data points with the logistic equation indicated in the legend of Figure 3 gave a maximum inhibition of 85%, reached at the concentration of 5  $\mu$ M, an  $EC_{50}$  of 0.8  $\mu$ M, and a coefficient of 2.37. Thus, the effect of ruthenium red on  $I_{Ca}$  is complex, as at least two interaction sites are involved in the blocking effect.

#### Effect of ruthenium red on the sodium current

The effects of ruthenium red were also tested on the sodium current ( $I_{Na}$ ) recorded at room temperature in low sodium-containing saline (30 mM). Figure 4A illustrates a typical time course of the effect of 10  $\mu$ M ruthenium red on the amplitude of the peak inward sodium current elicited by applying 20 ms depolarizing pulses from  $-100$  mV to  $-10$  mV at the rate of 0.1 Hz. The current traces corresponding to the control conditions (C) and after 5 min 30 of exposure to ruthenium red (RR) are shown in Figure 4Ba. At 10  $\mu$ M, ruthenium red markedly decreased  $I_{Na}$ , and noticeably slowed its inactivation time-course. This latter effect is better visualized in Figure 4Bb, in which the current traces have been normalized to their maximum. The reversibility of these effects of ruthenium red occurred slowly (about 80–90% of reversibility after 10 min of superfusion with drug-free saline). The mean blocking effect of 10  $\mu$ M ruthenium red was  $26.7 \pm 4.3\%$  ( $n = 8$ ). At 1  $\mu$ M, ruthenium red-induced block of  $I_{Na}$  was already significant and amounted to  $7.6 \pm 2.7\%$  ( $n = 3$ ). Slowing of the inactivation time course also occurred, but was much less marked (not shown).

The effects of ruthenium red were also assessed on the voltage-dependent properties of  $I_{Na}$ , Figure 5Aa illustrates

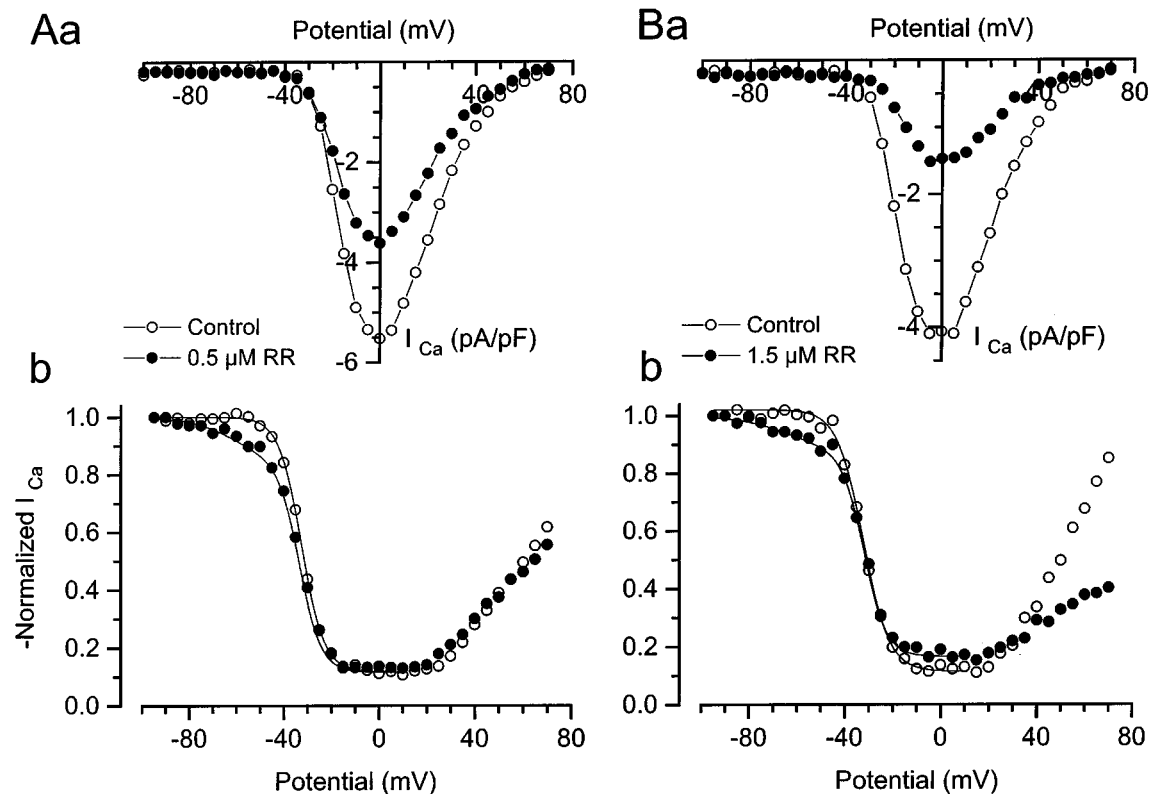


**Figure 2** Current-voltage relationships of the maximum peak inward calcium current in the absence (control) and in the presence of  $0.5 \mu\text{M}$  (Aa) and of  $1.5 \mu\text{M}$  (Ba) ruthenium red (RR) in two different cells (F7N03,  $C_m = 85.5 \text{ pF}$ , and E7N03,  $C_m = 78.3 \text{ pF}$ , respectively). Panels (b) show the steady-state inactivation curves of the calcium current determined with a classical two-steps protocol under the same experimental conditions, i.e., in the absence (control) and in the presence of  $0.5 \mu\text{M}$  (Ab) and of  $1.5 \mu\text{M}$  (Bb) ruthenium red. Same cells as in (Aa) and (Ba). One second inactivating prepulses were applied from a HP of  $-100 \text{ mV}$  to various potentials indicated on the abscissa scale, and the  $400 \text{ ms}$  test pulse to  $0 \text{ mV}$  was applied after an  $8 \text{ ms}$  repolarization interval to the HP. The amplitudes of the peak inward current during the test pulse were normalized to their respective maximum value and are plotted as a function of the inactivating potential.

families of sodium current traces recorded in control conditions and in the presence of  $10 \mu\text{M}$  ruthenium red, by applying  $20 \text{ ms}$  depolarizing pulses from  $-110 \text{ mV}$  to potentials between  $-50$  and  $+60 \text{ mV}$ , in  $5 \text{ mV}$  steps ( $-50$  to  $0 \text{ mV}$ ) and  $10 \text{ mV}$  steps ( $+10$  to  $+60 \text{ mV}$ ). The corresponding peak current-voltage relationships are shown in Figure 5Ab in control conditions and in the presence of  $10 \mu\text{M}$  ruthenium red. In control conditions,  $I_{\text{Na}}$  started to activate at around  $-50 \text{ mV}$ , was maximum at around  $-10 \text{ mV}$ , and had an apparent reversal potential between  $+45$  and  $+50 \text{ mV}$ . In the presence of ruthenium red,  $I_{\text{Na}}$  was decreased at all potentials, with no significant changes in the threshold and reversal potentials, nor in the potential at which the current was maximum.

The voltage-dependence of the steady-state inactivation of  $I_{\text{Na}}$  was determined with a classical double pulse protocol shown in inset in Figure 5Ba. A series of  $500 \text{ ms}$  inactivating prepulses were applied from  $-100 \text{ mV}$  to  $-20 \text{ mV}$  (in  $5 \text{ mV}$  steps), and a  $30 \text{ ms}$  test pulse from  $-100 \text{ mV}$  to  $-10 \text{ mV}$  was applied  $1 \text{ ms}$  after the termination of the inactivating prepulse. Figure 5Ba illustrates the current traces recorded during the test pulse in control conditions (left panel) and in the presence of  $10 \mu\text{M}$  ruthenium red (right panel). The amplitudes of the peak current recorded for each inactivating potential were normalized to that in the absence of an inactivating prepulse, and were plotted against the inactivating potential. These current-voltage relationships are shown in Figure 5Bb in control conditions and in the presence of  $10 \mu\text{M}$  ruthenium red.

In control conditions,  $I_{\text{Na}}$  inactivated between  $-95 \text{ mV}$  and  $-30 \text{ mV}$ , with a half-inactivating potential of  $-74 \text{ mV}$ . In the presence of  $10 \mu\text{M}$  ruthenium red, the voltage-dependence of the steady-state inactivation of  $I_{\text{Na}}$  was unchanged, except that the slope factor of the Boltzman relationship (see legend of Figure 5Bb) slightly increased from  $5$  to  $6 \text{ mV}$ . This small change in slope might induce an increase in the window Na current which could contribute to the increase of the inward current at the end of the depolarizing pulse.

The records presented in Figures 4 and 5 indicate that ruthenium red modifies the kinetics of inactivation of the sodium current, while the activation does not seem to be affected. These points were better assessed with three parameters: the time to peak current, the half-width of the transient current (i.e., the width of the transient at  $50\%$  of the peak amplitude) and the maximum inactivation rate (i.e., the maximum slope of the inactivation phase). The mean voltage-dependencies of these three parameters in control conditions and in the presence of  $10 \mu\text{M}$  ruthenium red are illustrated in Figure 6. Ruthenium red had no significant effect on the time to peak current, but significantly increased the width of the transient current (Figure 6a) for potentials between  $-30$  and  $+30 \text{ mV}$ , as expected from the data presented in Figure 4B and 5 showing a slowing of the inactivation phase of the Na current. In control conditions, the maximum inactivation rate of the sodium current increased with increasing voltages in the range  $-30$  to  $+10 \text{ mV}$  (Figure 6b), as expected from the voltage-dependent properties of the sodium current inactivation.

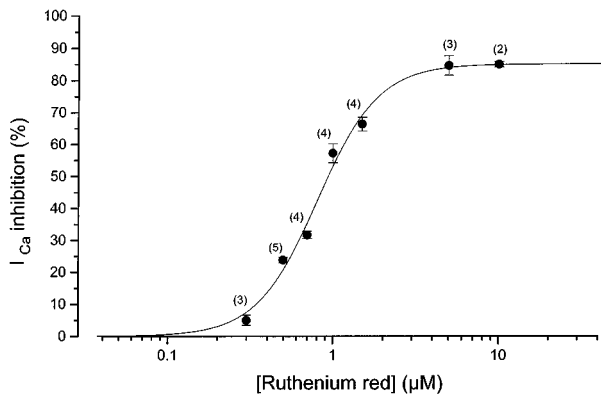


**Figure 3** Dose-response curve for the inhibitory effect of ruthenium red on the amplitude of the calcium current. Data points represent mean values of the effects of a single dose applied on several cells (number indicated near each point) and vertical lines represent s.e.mean. The smooth curve represents fit of the data points to the following logistic equation:  $\text{Inh} = \text{Inh}_{\text{max}} - [\text{Inh}_{\text{max}} / \{1 + ([\text{RR}]/[\text{EC}_{50}])^p\}]$  where Inh and  $\text{Inh}_{\text{max}}$  are, respectively, the observed inhibition of the calcium current at the concentration of RR of ruthenium red and the maximal inhibition,  $[\text{EC}_{50}]$  the ruthenium red concentration leading to 50% of  $\text{Inh}_{\text{max}}$ , and  $p$  a constant related to the slope of the sigmoidal curve. Best fit (no weighting) gave the following parameters:  $\text{Inh}_{\text{max}} = 85\%$ ,  $\text{EC}_{50} = 0.8 \mu\text{M}$ ,  $p = 2.37$ .

tion kinetics. However, in the presence of  $10 \mu\text{M}$  ruthenium red, the voltage-dependence of the maximum inactivation rate of the sodium current was almost abolished, suggesting the existence, also in control conditions, of a non voltage-dependent process of inactivation of the sodium current. It should be noted that the maximum inactivation rate of the calcium current was also not voltage-dependent in control conditions or in the presence of ruthenium red (not shown).

## Discussion

The main finding of our study is that ruthenium red is an effective blocker of both Ca and Na channels in heart cells, at concentrations used to assess intracellular Ca movements.

### Sensitivity of heart Ca channels to ruthenium red

Block of the Ca channels by ruthenium red is not really surprising, as a few studies have already demonstrated such a block in other types of preparations (Stimers & Byerly, 1982; Zholos *et al.*, 1991; Gomis *et al.*, 1994; Hamilton & Lundy, 1995). In guinea-pig ventricular heart cells, the sensitivity of  $I_{\text{Ca}}$  towards the blocking effect of ruthenium red ( $\text{EC}_{50} = 0.8 \mu\text{M}$ , this study) is almost similar to that observed with gadolinium ( $\text{EC}_{50}$  of  $1.4 \mu\text{M}$ ) in the same preparation (Lacampagne *et al.*,

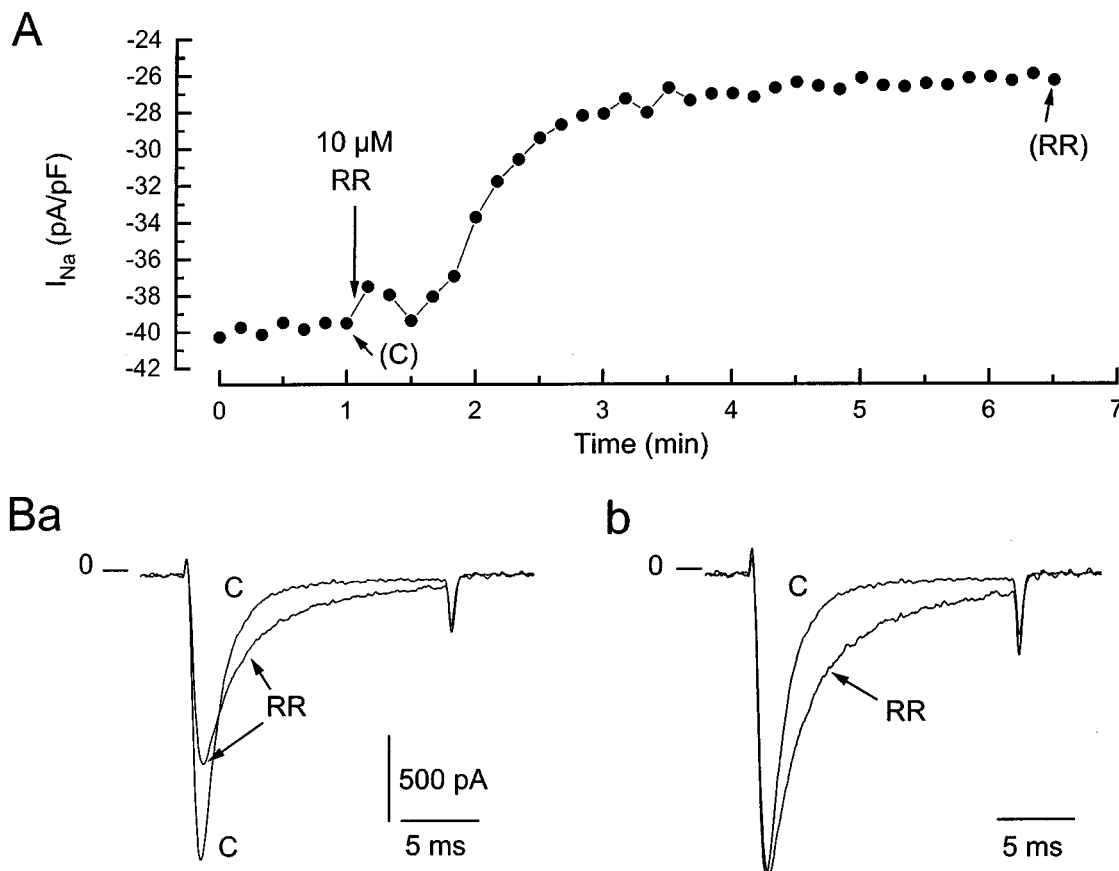


**Figure 4** Inhibitory effect of  $10 \mu\text{M}$  ruthenium red on the Na current. (A) Time-course of the effect of ruthenium red in a typical cell. The Na current was elicited by applying a 20 ms depolarizing pulse from  $-100 \text{ mV}$  to  $-10 \text{ mV}$ . (B) Current traces recorded at the time indicated in (A), in the absence (C) and in the presence (RR) of  $10 \mu\text{M}$  ruthenium red. In (a) are represented the actual traces, and in (b) current traces are normalized to their maximum, to visualize better the slowing of the kinetics of the Na current in the presence of ruthenium red. Cell E7O28,  $C_m = 40.5 \text{ pF}$ .

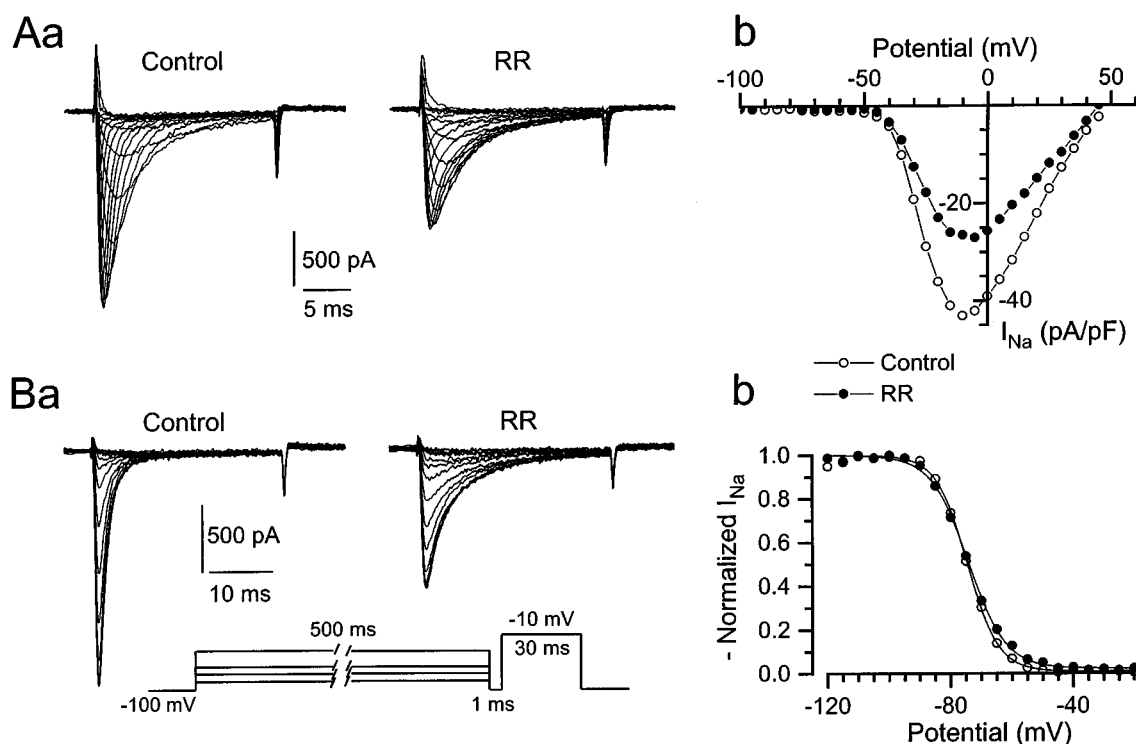


**Figure 5** Current-voltage relationships of the sodium current (A) and steady-state inactivation curves (B) in control conditions and in the presence of ruthenium red (RR). (Aa) Family of current traces elicited by applying 20 ms depolarizing pulses from  $-110$  mV to  $-50$  to  $0$  mV (5 mV step) and  $10$  to  $+60$  mV (10 mV step) in control conditions (left) and in the presence of  $10 \mu\text{M}$  ruthenium red (RR, right). Cell E7O28,  $C_m = 40.5$  pF, clamp time-constant =  $29.2 \mu\text{s}$ . (Ab) Corresponding current-voltage relationships of the maximum peak inward sodium current in the absence (control) and in the presence of  $10 \mu\text{M}$  ruthenium red. (Ba) Current traces of the sodium current recorded during the test pulse to  $-10$  mV, following the 500 ms inactivating prepulse, as illustrated by the protocol shown in inset, in control conditions (left) and in the presence of  $10 \mu\text{M}$  ruthenium red (RR, right). (Bb) Corresponding steady-state inactivation curves of the peak inward sodium current determined in the absence (control) and in the presence of  $10 \mu\text{M}$  ruthenium red. Five hundred milliseconds inactivating prepulses were applied from an HP of  $-100$  mV to various potentials indicated on the abscissa scale, and the 20 ms test pulse to  $-10$  mV was applied after a 1 ms repolarization interval to the HP. The amplitudes of the peak inward current during the test pulse were normalized to their respective maximum value and are plotted as a function of the inactivating potential. The smooth lines represent best fit of the data point with a Boltzman function of the form  $Y = 1/[1 + \exp\{-(V_{1/2}-V)/K\}]$ , where  $V_{1/2}$  represents the voltage at which half inactivation of the current occurs and  $K$  the slope factor. Control:  $V_{1/2} = -74.6$  mV,  $K = -5.07$ ; ruthenium red:  $V_{1/2} = 74.3$  mV,  $K = -6.08$  mV.

1994), although the maximum block induced by ruthenium red is only 85%, as compared to 100% block with gadolinium. When compared to other tissues, heart calcium channels are about ten times more sensitive to ruthenium red than those of snail neurones ( $EC_{50} = 5.4 \mu\text{M}$ , Stimers & Byerly, 1982), chromaffin cells ( $EC_{50} = 7 \mu\text{M}$ , Gomis *et al.*, 1994) and brain. In brain synaptosomes, ruthenium red has been shown to displace specifically bound  $\omega$ -CgTx ( $\omega$ -conotoxin GVIA) with an  $IC_{50}$  of  $2 \mu\text{M}$  in the rat and of  $6 \mu\text{M}$  in the chicken (Hamilton & Lundy, 1995), and to inhibit the K-stimulated Ca influx of the same preparations with an  $EC_{50}$  of  $69 \mu\text{M}$  and  $250 \mu\text{M}$ , respectively. Heart Ca channels also appear to be as sensitive to ruthenium red as those of smooth muscle cells isolated from the guinea-pig ileum (about 82% block at  $10 \mu\text{M}$ ; Zholos *et al.*, 1991; see their Figure 5A).

#### Mechanisms of Ca channel block

The rapid onset of current block we observed suggested that the main site of action of ruthenium red is located extracellularly. Block of Ca channels by ruthenium red cannot be explained by a screening of surface charges, since the voltage-dependence of the Ca current was not affected. Ruthenium red is a highly charged inorganic cation, which might quickly and strongly interact with the negatively charged

amino acid residues located at the outer mouth of the Ca channels, mostly with the carboxyl groups, which have been shown by Hess and Tsien (1984) to play a role in Ca permeation. Indeed, ruthenium red has been shown to react with ionizable carboxylic acid groups (Luft, 1971). Strong binding of ruthenium red is also suggested by the slow reversibility of its blocking effect at high concentrations. Binding of ruthenium red to phospholipids and fatty acids has also been demonstrated, as well as staining of the sarcoplasmic reticulum in muscle tissue (Luft, 1971). The second slow phase of current block by ruthenium red, associated with a slowing of the inactivation phase, might suggest an intracellular effect. Indeed, several studies have shown the presence of ruthenium red in the myoplasm of cardiac cells after exposure to this agent (Forbes & Sperelakis, 1979; Gupta *et al.*, 1988; Tanaka *et al.*, 1977). Recently, Viele and Betz (1995) have shown that the uptake of ruthenium red by endothelial cells was blocked by the calcium channel blocker flunarizine, suggesting that ruthenium red might enter the cell through voltage-dependent Ca channels. However, in heart cells, such a mechanism is unlikely for two reasons. Firstly, the size of a molecule of ruthenium red has been shown to either correspond to a sphere of  $11.3 \text{ \AA}$  in diameter (Luft, 1971), or to a more complex molecule of  $15 \text{ \AA}$  in length by  $8 \text{ \AA}$  in width (Gomis *et al.*, 1994), which is more than that of the radius of the non-hydrated Ca

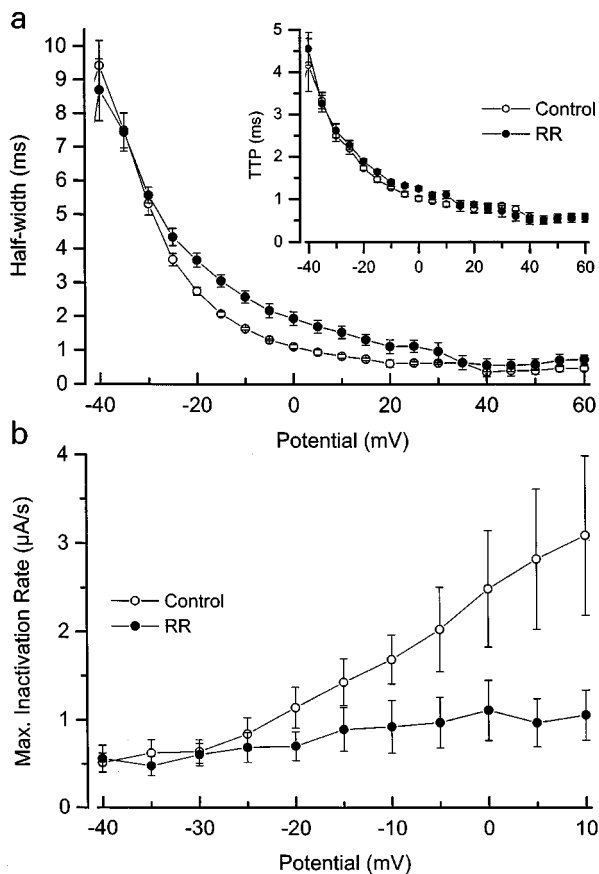


**Figure 6** Kinetics of the sodium current. (a) Voltage-dependence of the width of the transient sodium current at 50% of the peak amplitude in control conditions (control) and in the presence of  $10 \mu\text{M}$  ruthenium red (RR). Inset: the voltage dependence of the time to peak current under the same conditions. (b) Voltage-dependence of the maximum inactivation rate of the sodium current in control conditions and in the presence of  $10 \mu\text{M}$  ruthenium red for the same cells as in (a). The maximum inactivation rate was determined as the maximum slope of the inactivation phase of the sodium current. Data points shown are mean values observed in 5 cells, and the vertical lines represent s.e.mean.

ion itself ( $0.99 \text{ \AA}$ ), and also more than the minimal pore diameter of  $6 \text{ \AA}$  determined for the skeletal muscle Ca channel by McCleskey and Almers (1985). Secondly, it would be surprising that a charged molecule which blocks most of the Ca current could permeate the Ca channel themselves. In skeletal muscle fibre segments, intracellular application of ruthenium red by diffusion from the cut ends has been shown to very slowly depress the Ca current, in a way similar to that of the internal application of the Ca chelator BAPTA (Feldmeyer *et al.*, 1993). The existence of both extra- and intracellular sites of actions of ruthenium red might also be in agreement with the high value of the coefficient of the logistic equation (2.37) describing the dose-response curve of the block of the Ca current by ruthenium red (see Figure 3). The slow phase of current block by ruthenium red might also reflect a progressive dephosphorylation process of the channel protein, due to its calmodulin antagonist properties (Masuoka *et al.*, 1990). Moreover, calmodulin antagonists have been shown to block Na, Ca and K channels in cardiac myocytes directly (Klöcker & Isenberg, 1987; Kimura, 1993).

### Block and modification of sodium channels

Only three studies have shown so far, to our knowledge, an effect of ruthenium red on the sodium current. Indeed, it has been shown that ruthenium red slowed the inactivation kinetics of the sodium current in snail neurones (Stimers & Byerly, 1982), in the rat node of Ranvier (Neumcke *et al.*, 1987) and in neuroblastoma cells (Nosyreva *et al.*, 1988). In some respects, heart Na channels behave like those of rat and frog myelinated fibres, with respect to their sensitivity to ruthenium red, since in these preparations,  $10 \mu\text{M}$  ruthenium red induced about 35–40% block of the Na current (Neumcke *et al.*, 1987), as compared to the 27% block we found for the same dose. When compared to Ca current, blockade of the sodium current was slower (see Figures 1A and 4A) as no fast phase of block was present, and was also less pronounced. The mechanism by which ruthenium red partially blocked the Na current and slowed its kinetics of inactivation is not obvious, but might be related also to the competition between ruthenium red and calcium ions for common binding sites. Indeed, several ions including lanthanum, lanthanide and fluoride, known to compete with or to chelate calcium, have been found to decrease the Na current in heart cells and to slow down its inactivation time-course (Bustamante, 1987; Kohlhardt, 1991). However, if this were the case, this mechanism should not involve surface charge screening since we have found that the voltage-dependent properties of the Na current were not modified by ruthenium red. The blocking effect of ruthenium red on the Na current might also be related to its calmodulin antagonist properties, since several calmodulin antagonists have been found to block Na, Ca and K channels in ventricular and vascular myocytes (Klöcker & Isenberg, 1987; Kimura, 1993). Na channel activity in heart cells has been shown to be decreased by cyclicAMP-dependent phosphorylation (Schubert *et al.*, 1989; Ono *et al.*, 1989, 1993; Sunami *et al.*, 1991; Muramatsu *et al.*, 1994). Although ruthenium red might increase intracellular cyclicAMP levels through its inhibitory action on the Ca-dependent cyclic nucleotide phosphodiesterase (Masuoka *et al.*, 1990), such a mechanism is probably not responsible for the blocking effect we observed, since phosphorylation of the Na channels has been shown to modify their voltage-dependence (negative shift of the steady-state inactivation curve; Schubert *et al.*, 1989; Ono *et al.*, 1989, 1993; Muramatsu *et al.*, 1994), whereas ruthenium red did not.

### Can the block of Ca and Na channels contribute to the beneficial effect of ruthenium red in ischaemia-reperfusion?

One of the deleterious effects occurring during ischaemia is the Ca overload. Although the protective effect of ruthenium red in ischaemia has been attributed mostly to the prevention of mitochondrial Ca overload and free radicals production (Grover *et al.*, 1990; Figueredo *et al.*, 1991; Benzi & Lerch, 1992; Tan, 1993; Leperre *et al.*, 1995; Miyamae *et al.*, 1996), the inhibition of the Ca current by ruthenium red would also contribute to decrease the cytoplasmic Ca concentration. However, it should be noted that the partial block of both Na and Ca channels could enhance slow conduction and thus re-entry phenomena occurring in partially depolarized ischaemic myocardium.

## References

- BENZI, R.H. & LERCH, R. (1992). Dissociation between contractile function and oxidative metabolism in postischemic myocardium. Attenuation by ruthenium red administered during reperfusion. *Circ. Res.*, **71**, 567–576.
- BEZANILLA, F. & ARMSTRONG, C.M. (1977). Inactivation of the sodium channel. I. Sodium current experiments. *J. Gen. Physiol.*, **70**, 549–566.
- BUSTAMANTE, J.O. (1987). Modification of sodium channel currents by lanthanum and lanthanide ions in human heart cells. *Can. J. Physiol. Pharmacol.*, **65**, 591–597.
- CHAMBERLAIN, B.K., VOLPE, P. & FLEISCHER, S. (1984). Inhibition of calcium-induced calcium release from purified cardiac sarcoplasmic reticulum vesicles. *J. Biol. Chem.*, **259**, 7547–7553.
- DING, J. & KASAI, M. (1996). Analysis of multiple conductance states observed in  $\text{Ca}^{2+}$  release channel of sarcoplasmic reticulum. *Cell Struct. Funct.*, **21**, 7–15.
- FELDMAYER, D., MELZER, W., POHL, B. & ZÖLLNER, P. (1993). A possible role of sarcoplasmic  $\text{Ca}^{2+}$  release in modulating the slow  $\text{Ca}^{2+}$  current of skeletal muscle. *Pflügers Arch.*, **425**, 54–61.
- FIGUEREDO, V.M., DRESDNER, K.P., JR., WOLNEY, A.C. & KELLER, A.M. (1991). Postischemic reperfusion injury in the isolated rat heart: effect of ruthenium red. *Cardiovasc. Res.*, **25**, 337–342.
- FORBES, M.S. & SPERELAKIS, N. (1979). Ruthenium red staining of skeletal and cardiac muscles. *Cell Tissue Res.*, **200**, 267–382.
- GAGOV, H.S., DURIDANOVA, D.B., BOEV, K.K. & DANIEL, E.E. (1994). L-type calcium channels may fill directly the IP3-sensitive calcium store. *Gen. Physiol. Biophys.*, **13**, 75–84.
- GOMIS, A., GUTIERREZ, L.M., SALA, F., VINIEGRA, S. & REIG, J.A. (1994). Ruthenium red inhibits selectively chromaffin cell calcium channels. *Biochem. Pharmacol.*, **47**, 225–231.
- GRIFFITHS, E.J. (1997). Ruthenium red as an inhibitor of mitochondrial  $\text{Ca}^{2+}$  uptake in single adult rat cardiomyocytes. *J. Physiol.*, **504**, 96P.
- GROVER, G.J., DZWONCZYK, S. & SLEPH, P.G. (1990). Ruthenium red improves postischemic contractile function in isolated rat hearts. *J. Cardiovasc. Pharmacol.*, **16**, 783–789.
- GUPTA, M.P., INNES, I.R. & DHALLA, N.S. (1988). Responses of contractile function to ruthenium red in rat heart. *Am. J. Physiol.*, **255**, H1413–H1420.
- HAMILTON, M.G. & LUNDY, P.M. (1995). Effect of ruthenium red on voltage-sensitive  $\text{Ca}^{++}$  channels. *J. Pharmacol. Exp. Ther.*, **273**, 940–947.
- HESS, P. & TSIEH, R.W. (1984). Mechanism of ion permeation through calcium channels. *Nature*, **309**, 453–456.
- KIMURA, J. (1993). Effects of various calmodulin antagonists on Na/Ca exchange current of single ventricular cells of guinea-pig. *Pflügers Arch.*, **424**, 523–528.
- KLÖCKNER, U. & ISENBERG, G. (1987). Calmodulin antagonists depress calcium and potassium currents in ventricular and vascular myocytes. *Am. J. Physiol.*, **253**, H1601–H1611.
- KOHLHARDT, M. (1991). Gating properties of cardiac  $\text{Na}^{+}$  channels in cell-free conditions. *J. Membr. Biol.*, **122**, 11–21.
- LACAMPAGNE, A., GANNIER, F., ARGIBAY, J., GARNIER, D. & LE GUENNEC, J.-Y. (1994). The stretch-activated ion channel blocker gadolinium also blocks L-type calcium channels in isolated ventricular myocytes of the guinea-pig. *Biochim. Biophys. Acta*, **1191**, 205–208.
- LE GUENNEC, J.-Y., PEINEAU, N., ESNARD, F., LACAMPAGNE, A., GANNIER, F., ARGIBAY, J., GAUTHIER, F. & GARNIER, D. (1993). A simple method for calibrating collagenase/pronase E ratio to optimize heart cell isolation. *Biol. Cell*, **79**, 161–165.
- LEPERRE, A., MILLART, H., PREVOST, A., TRENQUE, T., KANTE-LIP, J.P. & KEPPLER, B.K. (1995). Compared effects of ruthenium red and cis  $[\text{Ru}(\text{NH}_3)_4\text{Cl}_2]\text{Cl}$  on the isolated ischaemic-reperfused rat heart. *Fundam. Clin. Pharmacol.*, **9**, 545–553.
- LUFT, J.H. (1971). Ruthenium red and violet. I. Chemistry, purification, methods of use for electron microscopy and mechanism of action. *Anat. Rec.*, **171**, 347–368.
- MA, J. (1993). Block by ruthenium red of the ryanodine-activated calcium release channel of skeletal muscle. *J. Gen. Physiol.*, **102**, 1031–1056.
- MACK, W.M., ZIMANYI, I. & PESSAH, I.N. (1992). Discrimination of multiple binding sites for antagonists of the calcium release complex of skeletal and cardiac sarcoplasmic reticulum. *J. Pharmacol. Exp. Ther.*, **262**, 1028–1037.
- MASUOKA, H., ITO, M., NAKANO, T., NAKA, M. & TANAKA, T. (1990). Effects of ruthenium red on activation of  $\text{Ca}^{2+}$ -dependent cyclic nucleotide phosphodiesterase. *Biochem. Biophys. Res. Commun.*, **169**, 315–322.
- MCCLESKEY, E.W. & ALMERS, W. (1985). The Ca channel in skeletal muscle is a large pore. *Proc. Natl. Acad. Sci. U.S.A.*, **82**, 7149–7153.
- MIYAMAE, M., CAMACHO, S.A., WEINER, M.W. & FIGUEREDO, V.M. (1996). Attenuation of postischemic reperfusion injury is related to prevention of  $[\text{Ca}^{2+}]_m$  overload in rat hearts. *Am. J. Physiol.*, **271**, H2145–H2153.
- MOORE, C.L. (1971). Specific inhibition of mitochondrial  $\text{Ca}^{++}$  transport by ruthenium red. *Biochim. Biophys. Res. Commun.*, **42**, 298–305.
- MURAMATSU, H., KIYOSUE, T., ARITA, M., ISHIKAWA, T. & HIDAKA, H. (1994). Modification of cardiac sodium current by intracellular application of cAMP. *Pflügers Arch.*, **426**, 146–154.
- NAGASAKI, K. & FLEISCHER, S. (1989). Modulation of the calcium release channel of sarcoplasmic reticulum by adriamycin and other drugs. *Cell Calcium*, **10**, 63–70.
- NEUMCKE, B., SCHWARZ, J.R. & STAMPFLI, R. (1987). A comparison of sodium currents in rat and frog myelinated nerve: normal and modified sodium inactivation. *J. Physiol.*, **382**, 175–191.
- NOSYREVA, E.D., GRISHCHENKO, I.I. & NEGULIAEV, Iu.A. (1988). Effect of ruthenium red on the sodium channel inactivation of neuroblastoma cells. *Neirofiziologia*, **20**, 131–134.
- ONO, K., FOZZARD, H.A. & HANCK, D.A. (1993). Mechanism of cAMP-dependent modulation of cardiac sodium channel current kinetics. *Circ. Res.*, **72**, 807–815.
- ONO, K., KIYOSUE, T. & ARITA, M. (1989). Isoproterenol, DBcAMP, and forskolin inhibit cardiac sodium current. *Am. J. Physiol.*, **256**, C1131–C1137.
- RIZZUTO, R., BERNARDI, P., FAVARON, M. & AZZONE, G.F. (1987). Pathways for calcium efflux in heart and liver mitochondria. *Biochem. J.*, **246**, 271–277.
- SCHUBERT, B., VANDONGEN, A.M.J., KIRSCH, G.E. & BROWN, A.M. (1989).  $\beta$ -Adrenergic inhibition of cardiac sodium channels by dual G-protein pathways. *Science*, **245**, 516–519.
- SORDHAL, L.A. (1975). Effect of magnesium, ruthenium red and the antibiotic ionophore A23187 on initial rates of calcium uptake and release by heart mitochondria. *Arch. Biochem. Biophys.*, **167**, 104–115.
- STIMERS, J.R. & BYERLY, L. (1982). Slowing of sodium current inactivation by ruthenium red in snail neurones. *J. Gen. Physiol.*, **80**, 485–497.
- SUNAMI, A., FAN, Z., NAKAMURA, F., NAKA, M., TANAKA, T., SAWANABORI, T. & HIRAOKA, M. (1991). The catalytic subunit of cyclic AMP-dependent protein kinase directly inhibits sodium channel activities in guinea-pig ventricular myocytes. *Pflügers Arch.*, **419**, 415–417.
- TAN, Z.T. (1993). Ruthenium red, ribose, and adenine enhance recovery of reperfused heart. *Coron. Artery Dis.*, **4**, 305–309.
- TANAKA, E., KAWAI, M., KURIHARA, S., HOTTA, Y. & SOJI, T. (1997). Effects of ruthenium red on the cellular functions and ultrastructure in intact ferret ventricular muscles. *Jpn. J. Physiol.*, **47**, 273–281.
- VASINGTON, F.D., GAZZOTTI, P., TIOZZO, R. & CARAFOLI, E. (1972). The effect of ruthenium red on  $\text{Ca}^{2+}$  transport and respiration in rat liver mitochondria. *Biochem. Biophys. Acta*, **256**, 43–54.
- VIELE, D. & BETZ, E. (1995). Effect of the calcium entry blocker, flunarizine, on ruthenium red uptake by endothelial cells following acute electrical stimulation of rabbit carotid arteries. *Basic Res. Cardiol.*, **80**, 59–65.
- VITES, A.M. & PAPPANO, A.J. (1994). Distinct modes of inhibition by ruthenium red and ryanodine of calcium-induced calcium release in avian atrium. *J. Pharmacol. Exp. Ther.*, **268**, 1476–1484.
- ZHOLOS, A.V., BAIDAN, L.V. & SHUBA, M.F. (1991). The inhibitory action of caffeine on calcium currents in isolated intestinal smooth muscle cells. *Pflügers Arch.*, **419**, 267–273.
- ZHU, Y. & NOSEK, T.M. (1992). Ruthenium red affects the contractile apparatus but not sarcoplasmic reticulum  $\text{Ca}^{2+}$  release of skinned papillary muscle. *Pflügers Arch.*, **420**, 255–258.

(Received January 13, 1998  
Accepted February 24, 1998)